

Field driven ferromagnetic phase nucleation and propagation in antiferromagnetically coupled multilayer films with perpendicular anisotropy

T. Hauet, C. M. Günther, O. Hovorka, A. Berger, M.-Y. Im et al.

Citation: [Appl. Phys. Lett.](#) **93**, 042505 (2008); doi: 10.1063/1.2961001

View online: <http://dx.doi.org/10.1063/1.2961001>

View Table of Contents: <http://apl.aip.org/resource/1/APPLAB/v93/i4>

Published by the [American Institute of Physics](#).

Additional information on *Appl. Phys. Lett.*

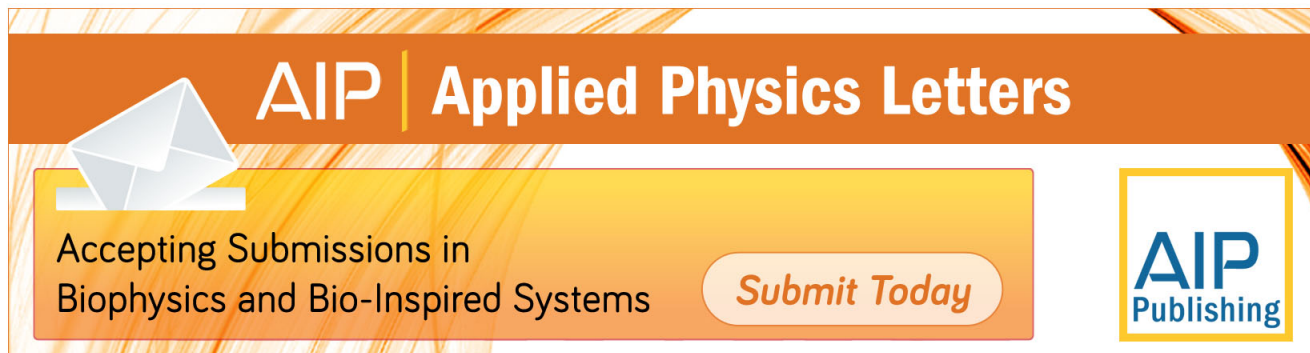
Journal Homepage: <http://apl.aip.org/>

Journal Information: http://apl.aip.org/about/about_the_journal

Top downloads: http://apl.aip.org/features/most_downloaded

Information for Authors: <http://apl.aip.org/authors>

ADVERTISEMENT



AIP | Applied Physics Letters

Accepting Submissions in
Biophysics and Bio-Inspired Systems

Submit Today

AIP
Publishing

Field driven ferromagnetic phase nucleation and propagation in antiferromagnetically coupled multilayer films with perpendicular anisotropy

T. Hauet,^{1,a)} C. M. Günther,² O. Hovorka,³ A. Berger,³ M.-Y. Im,⁴ P. Fischer,⁴ T. Eimüller,⁵ and O. Hellwig¹

¹San Jose Research Center, Hitachi Global Storage Technologies, San Jose, California 95135, USA

²BESSY GmbH, D-12489 Berlin, Germany

³CIC nanoGUNE Consolider, Donostia, San Sebastian E20009, Spain

⁴Center for X-Ray Optics, Lawrence Berkeley National Laboratory, Berkeley, California 94720, USA

⁵Junior Research Group Magnetic Microscopy, Ruhr-University of Bochum, D-44780 Bochum, Germany

(Received 22 February 2008; accepted 1 July 2008; published online 28 July 2008)

We investigate the reversal process in $\{[\text{Co}/\text{Pt}]_{X-1}\text{Co}/\text{Ru}\} \times 16/[\text{Co}/\text{Pt}]_X$ multilayer films by magnetometry and magnetic transmission x-ray microscopy. After demagnetization, a stable one-dimensional ferromagnetic (FM) stripe domain phase (tiger-tail phase) for a thick sample ($X=7$) is imaged, while metastable sharp antiferromagnetic domain walls are observed in the remanent state for a thinner stack sample ($X=6$). When applying an external magnetic field the sharp domain walls of the thinner sample gradually transform into the FM phase via separate nucleation of many isolated FM domains all along the domain boundary. We present energy calculations that reveal the underlying energetics driving the overall reversal mechanism. © 2008 American Institute of Physics. [DOI: 10.1063/1.2961001]

Strong perpendicular anisotropy Co/Pt multilayer systems that are antiferromagnetically coupled via thin Ru or NiO interlayers have recently been proposed as model systems to study the competition between local interlayer exchange and long-range dipolar interactions.¹⁻⁴ The observation of magnetic structure transformations induced by extrinsic parameters such as a varying magnetic field provides the possibility to investigate the delicate energy balance in such systems.⁵⁻⁷ Previous experiments used mostly magnetic force microscopy as microscopic characterization method, which allows for the detection of surface stray fields only, but never completely eliminates image artifacts due to tip/sample interactions.^{2,4,5}

In this letter, we present a study of the domain boundary structure in $\{[\text{Co}/\text{Pt}]_{X-1}\text{Co}/\text{Ru}\} \times 16/[\text{Co}/\text{Pt}]_X$ antiferromagnetic (AF)-coupled multilayers. We report on magnetometry measurements and magnetic transmission x-ray microscopy (MTXM) imaging of two similar samples with $X=6$ and $X=7$ forming different remanent AF domain wall structures after demagnetization, one ($X=6$) revealing sharp AF domain walls and the other one ($X=7$) one-dimensional ferromagnetic (FM) stripe domain walls (tiger tails).^{1,2,5} We explore the evolution of their magnetic states in an external field and compare our experimental data with corresponding energy calculations.

The exact sample structure we use is $\{[\text{Co}(4 \text{ \AA})/\text{Pt}(7 \text{ \AA})]_{X-1}/\text{Co}(4 \text{ \AA})/\text{Ru}(9 \text{ \AA})\} \times 16/[\text{Co}(4 \text{ \AA})/\text{Pt}(7 \text{ \AA})]_X$ with $X=6$ and $X=7$, referred to as samples X6 and X7, respectively. The multilayers were deposited by DC magnetron sputtering onto x-ray transparent SiN_x membranes at ambient temperature. We use a commercial vibrating sample magnetometer to measure the magnetization versus field behavior along the surface normal.

Figure 1(a) shows hysteresis loops of sample X6 measured at 300 K. Starting from positive saturation, the first

drop in magnetization corresponds to the synchronized reversal of 8 of the overall 17 Co/Pt stacks, such that the sample reaches a uniform AF state at remanence. Due to the odd number of stacks only one type of AF domain is populated, with the top and bottom stacks remaining in the previous saturation direction. When applying negative fields to the uniform AF remanent state we observe initially the reversal of the two surface stacks and then the seven remaining bulk stacks that switch in a second synchronized reversal. The corresponding behavior of sample X7 is similar [Fig. 1(b)] except that the surface stack reversal is less well visible.⁵

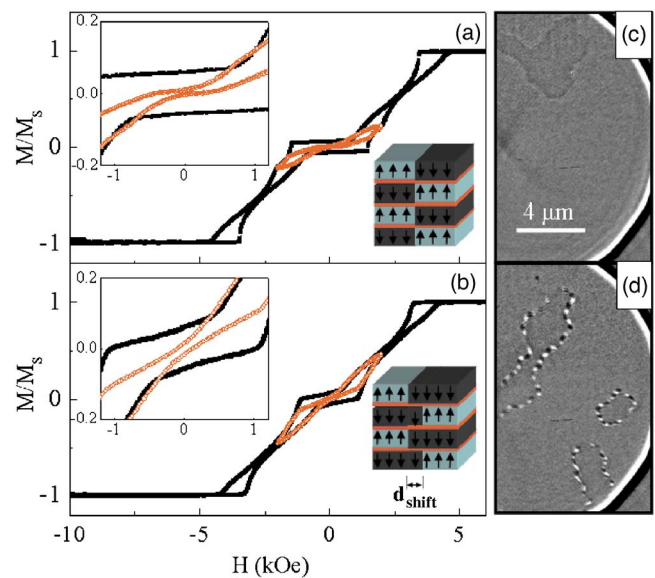


FIG. 1. (Color online) Normalized magnetization plotted vs external field for sample X6 (a) and sample X7 (b) at 300 K. The solid symbols mark the major loop data between ± 10 kOe, while the open symbols were measured between ± 2 kOe after out-of-plane demagnetization. The insets show the range between ± 1.2 kOe in more detail. (c) and (d) are MTXM images of the demagnetized state of samples X6 and X7, respectively, showing AF domains with different domain wall structures.

^{a)}Electronic mail: thomas.hauet@hitachigst.com.

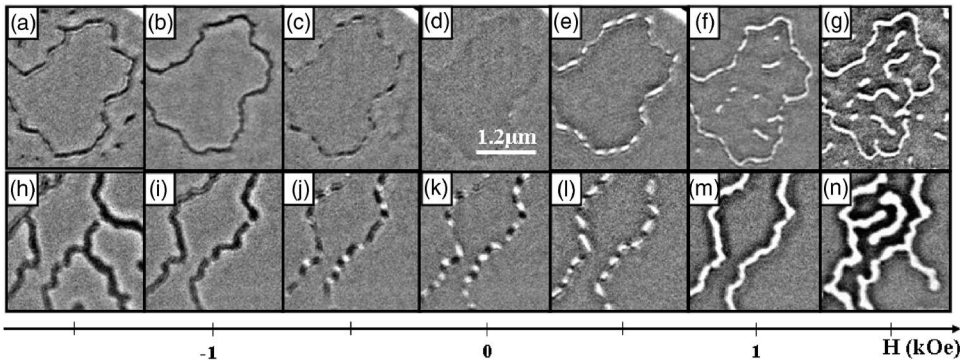


FIG. 2. (Double column) MTXM images of sample X6 (a)–(g) and sample X7 (h)–(n) as a function of applied field.

To achieve additional microscopic understanding of this behavior, we performed high-resolution MTXM experiments to image the domain structure of samples X6 and X7 close to the magnetic phase transition reported earlier.^{1,5} Exploiting x-ray magnetic circular dichroism as magnetic contrast mechanism, we use Fresnel zone plates as optical elements, which allow imaging lateral magnetic structures such as domains or domain walls with spatial resolution down to 15 nm.^{8,9} Experiments were done at the Advanced Light Source in Berkeley, CA at beamline 6.1.2.^{8,10} Figures 1(c) and 1(d) present remanent MTXM images measured at 300 K at the Co- L_3 absorption edge after out-of-plane demagnetization of samples X6 and X7, respectively. We observe a weak contrast between different AF domains due to the overall odd number of Co/Pt stacks, which prevents a perfect compensation of the magnetization. For the thinner stack sample X6 [Fig. 1(c)], we observe sharp domain walls between the two regions of opposite AF order (up-down-up... versus down-up-down...), as illustrated in the inset of Fig. 1(a). Here the domain walls of the individual stacks are all vertically aligned with each other, thus minimizing the AF interstack exchange energy. The remanent magnetization is zero due to the 50/50 domain state, as shown in the inset of Fig. 1(a). This is no longer the case for the thicker sample X7, which shows a nonzero magnetization [Fig. 1(b)] and a FM stripe domain wall formed by alternately shifted stacks, thus minimizing the dipolar energy [Fig. 1(d)]. In addition a one-dimensional FM stripe pattern is stabilized along the AF domain walls (tiger tails) due to intra-domain wall dipolar fields.^{2,5}

When applying external magnetic fields to the remanent stripe domain wall state of sample X7 [Figs. 2(h)–2(n)], wall segments magnetized along the external field grow at the expense of the oppositely magnetized parts until a uniform FM stripe along the AF domain boundary is obtained at about ± 1 kOe [Figs. 2(i) and 2(m)]. The FM stripe width d_{shift} [inset of Fig. 1(b)] increases slightly with growing external field, from 160 nm at remanence to 200 nm at 1 kOe. On the contrary, when applying external magnetic fields to sample X6 [Figs. 2(a)–2(f)], sharp domain walls are preserved until about 250 Oe. Above this value a phase of much stronger contrast appears along the domain boundary [Fig. 2(c) and 2(e)] indicating the formation of FM order.^{2,5} The FM phase nucleates all along the AF domain wall until a continuous FM band is formed [Figs. 2(b) and 2(f)]. Individual domain walls of each sublayer stack are no longer vertically aligned, but exhibit an alternating shift to the left and to the right with respect to the zero field domain wall position. We find that d_{shift} is about 120 nm at 0.5 kOe.

To qualitatively understand the observed behavior, we calculate the FM domain wall profiles at different external fields, and determine d_{shift}^0 as an equilibrium value by energy minimization. For this purpose, we considered a simple one-dimensional model picture, in which the domain wall in each Co/Pt stack was assumed to be a Bloch-type wall with a fixed width of 25 nm.¹¹ Calculation details and parameter values can be found in Refs. 1 and 5. The total energy profiles, which include exchange, dipolar, and Zeeman energy contributions, calculated for samples X6 and X7 are shown in Figs. 3(a) and 3(b). At low enough fields, there exist two energy minima for both samples: a local energy minimum for $d_{\text{shift}}=0$ nm, corresponding to the vertically aligned sub-stack domain walls, and the global energy minimum at $d_{\text{shift}}>0$ nm, which represents the FM phase of characteristic width d_{shift}^0 . The field dependence of the activation barrier E_{act} separating the minima is plotted in Fig. 3(c). As can be noticed, E_{act} at zero field (remanence) is almost doubled for sample X6 and therefore the transition probability out of the no-shift state is considerably reduced in comparison to sample X7. As a result the thinner sample X6 is likely to remain trapped in the metastable no-shift phase [Fig. 2(d)], after being initially populated during the demagnetization procedure. At certain external field values, E_{act} reduces to zero for both samples. For example, for sample X6, the activation barrier disappears at about 0.5 kOe [Fig. 3(c)] and is accompanied by the forced emergence of the FM phase [Fig. 2(e)]. Increasing the field further results only in more pronounced widening of the FM domains [Fig. 3(d)]. Hence, our simple model qualitatively describes the observed behavior.

As shown in Fig. 2, both samples behave rather similarly at fields above 1 kOe where the FM boundary not only broadens but also additional FM domains nucleate and propagate into the AF regions. In previous publications with only a few magnetic stacks, i.e., significantly lower dipolar interaction, a continuous widening of the FM domain boundary phase was observed toward saturation.^{3,4} Here, due to the overall thick structures, dipolar fields prevent FM domain growth beyond a certain characteristic stripe domain width. For both samples, the overall odd number of Co/Pt stacks favors nucleating all-up domains inside one of the two AF domain regions since the Zeeman energy is slightly lower for that state [compare Figs. 2(a), 2(g), 2(h), and 2(n)]. Comparing the calculated d_{shift}^0 and measured d_{shift} values, we obtain agreement for fields up to 1 kOe, as shown in Fig. 3(d). For higher fields, however, due to the formation of the labyrinth domain structure, the experimentally observed increase in d_{shift} is slower than the calculated exponential expansion,

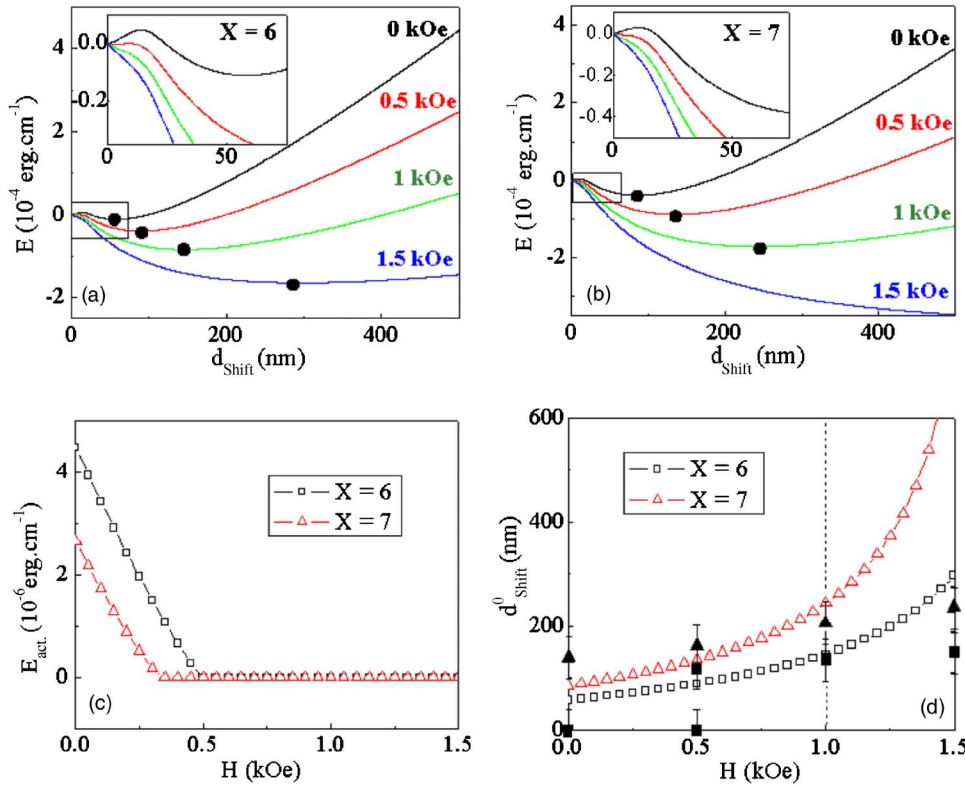


FIG. 3. (Color online) [(a) and (b)] Calculated total energy density for an AF domain wall as a function of the FM width d_{shift} for $X=6$ (a) and $X=7$ (b) for different field values as indicated. Inset: Close up of the region with small d_{shift} . Black dots are a guide to the eye for the energy minimum position. (c) Energy barrier height with respect to the first energy minimum as a function of field. (d) Calculated optimum d_{shift}^0 as a function of field (open symbols) compared with FM domain widths d_{shift} extracted from Fig. 2 (solid symbols).

since capturing such two-dimensional behavior is outside the scope of our one-dimensional model.

In conclusion, our study reveals the detailed behavior of FM domain nucleation and evolution in two thick $\{[\text{Co}/\text{Pt}]_{X-1}\text{Co}/\text{Ru}\} \times 16/[\text{Co}/\text{Pt}]_X$ multilayers after out-of-plane demagnetization. We use MTXM to image the AF domain boundary structure in external magnetic fields. For $X=7$ we observe a stable “tiger-tail” pattern at remanence, while for $X=6$ a metastable sharp AF domain wall structure is preferred. In addition within a certain field range we observe many separate nucleation sites of the FM phase all along the sharp AF domain boundary of the thinner $X=6$ sample. Thus our images directly reveal the transformation of the domain wall structure with increasing external field as well as the possible coexistence of sharp AF domain walls and the FM stripe phase. Additional calculations elucidate the reversal behavior and the delicate energy balance of perpendicular AF-coupled multilayer systems in external magnetic fields.

We thank E. E. Fullerton and B. D. Terris for helpful discussions. This work was partially supported by Lavoisier Fellowship and by Deutsche Forschungsgemeinschaft (DFG) via Project No. SFB491-N1. The soft x-ray microscope was supported by the Director, Office of Science, Office of Basic Energy Sciences, Materials Sciences and Engineering Divi-

sion, of the U.S. Department of Energy. Work at nanoGUNE is supported by the Department of Industry, Trade and Tourism of the Basque Government and the Provincial Council of Gipuzkoa under the ETORTEK Program, Project No. IE06-172, as well as from the Spanish Ministry of Science and Education under the Consolider-Ingenio 2010 Program, Project No. CSD2006-53.

¹O. Hellwig, T. L. Kirk, J. B. Kortright, A. Berger, and E. E. Fullerton, *Nat. Mater.* **2**, 112 (2003).

²O. Hellwig, A. Berger, and E. E. Fullerton, *Phys. Rev. Lett.* **91**, 197203 (2003).

³A. Baruth, L. Yuan, J. D. Burton, K. Janicka, E. Y. Tsymbal, S. H. Liou, and S. Adenwalla, *Appl. Phys. Lett.* **89**, 202505 (2006).

⁴Y. Fu, W. Pei, J. Yuan, T. Wang, T. Hasegawa, T. Washiya, H. Saito, and S. Ishio, *Appl. Phys. Lett.* **91**, 152505 (2007).

⁵O. Hellwig, A. Berger, J. B. Kortright, and E. E. Fullerton, *J. Magn. Magn. Mater.* **319**, 13 (2007).

⁶K. Janicka, J. D. Burton, and E. Y. Tsymbal, *J. Appl. Phys.* **101**, 113921 (2007).

⁷N. S. Kiselev, I. E. Dragunov, U. K. Rossler, and A. N. Bogdanov, *Appl. Phys. Lett.* **91**, 132507 (2007).

⁸P. Fischer, D.-H. Kim, W. Chao, J. A. Liddle, E. H. Anderson, and D. T. Attwood, *Mater. Today* **9**, 26 (2006).

⁹W. Chao, B. H. Harteneck, J. A. Liddle, E. H. Anderson, and D. T. Attwood, *Nature (London)* **435**, 1210 (2005).

¹⁰P. Fischer, *Curr. Opin. Solid State Mater. Sci.* **7**, 173 (2003).

¹¹O. Hellwig, G. P. Denbeaux, J. B. Kortright, and E. E. Fullerton, *Physica B* **336**, 136 (2003).